

## Supplementary Materials for

### Optoelectronic control of single cells using organic photocapacitors

Marie Jakešová, Malin Silverå Ejneby, Vedran Đerek, Tony Schmidt, Maciej Gryszel, Johan Brask, Rainer Schindl, Daniel T. Simon, Magnus Berggren, Fredrik Elinder, Eric Daniel Głowacki\*

\*Corresponding author. Email: [eric.glowacki@liu.se](mailto:eric.glowacki@liu.se)

Published 5 April 2019, *Sci. Adv.* **5**, eaav5265 (2019)  
DOI: 10.1126/sciadv.aav5265

#### The PDF file includes:

Supporting Note 1. Photofaradaic reactions: Quantification of H<sub>2</sub>O<sub>2</sub> production.

Supporting Note 2. Numerical modeling of the OEPC/oocyte interface.

Table S1. Results of H<sub>2</sub>O<sub>2</sub> photogeneration.

Fig. S1. Illustration of photocapacitive versus photofaradaic behavior in OEPCs.

Fig. S2. SEM micrographs comparing control samples of ITO/H<sub>2</sub>Pc/PTCDI.

Fig. S3. SEM micrographs of samples subjected to 178 days of light pulse stress.

Fig. S4. 2D representation of the electrolyte/oocyte/photocapacitor system.

Fig. S5. A 3D representation of the oocyte/photocapacitor model.

Fig. S6. Comparison of voltage transients in the case of light intensity ramps with a standard square light pulse.

#### Other Supplementary Material for this manuscript includes the following:

(available at [advances.sciencemag.org/cgi/content/full/5/4/eaav5265/DC1](https://advances.sciencemag.org/cgi/content/full/5/4/eaav5265/DC1))

Movie S1 (.avi format). Animation of evolution of transient potentials and membrane potentials during a 1-ms illumination pulse for an oocyte on top of an OEPC.

**Supporting Note 1. Photofaradaic reactions: Quantification of H<sub>2</sub>O<sub>2</sub> production.**

An additional important consideration is controlling for undesired faradaic processes. In our first version of the OEPC, an Au back electrode was used. We tested if the H<sub>2</sub>Pc/PTCDI device stack on Au produced photofaradaic cathodic processes, and found purely capacitive current in a photoelectrochemical experiment. That experiment did not however address the possibility of anodic reactions on the Au, since the Au was not exposed to the electrolyte. We hypothesized that if anodic reactions were possible on the back electrode, a cathodic process on PTCDI could complete the redox cycle. We based this supposition on our recent finding that PTCDI can cathodically reduce oxygen to hydrogen peroxide (36). This turned out indeed to be the case. OEPC devices with Au back electrodes were immersed in aerated artificial cerebrospinal fluid and illuminated with pulsed red light (5 ms pulses, 200 ms interval, 6 mW/mm<sup>2</sup> intensity) produced hydrogen peroxide with concentration rising at a rate of 4 μM/hour. The hydrogen peroxide was quantified according to procedures we have elaborated recently (36). The experimental results for Au- and ITO-based OEPCs is shown in the tables below. Peroxide is the result of oxygen reduction on the PTCDI layer, while the redox reaction is completed via anodic oxidation of one of the many easily oxidizable electron-donors present in artificial cerebrospinal fluid, such as glucose. While Au is known to be a fairly active faradaic electrode, ITO is reported to have a large inert potential window. Moreover, the ITO is modified with a monolayer of *n*-octyltriethoxysilane. This turned out to be a critical difference. The identical experiment for peroxide evolution yielded no detectable peroxide when ITO was used as the back electrode. This indicates that the device stack with ITO/H<sub>2</sub>Pc/PTCDI is truly photocapacitive.

**Table S1. Results of H<sub>2</sub>O<sub>2</sub> photogeneration.** For two OEPCs with Au back electrodes, compared with one with an ITO back electrode. No detectable peroxide was formed with ITO, while Au resulted in substantial quantities.

LED operation mode	sample	time [h]	C H <sub>2</sub> O <sub>2</sub> [μM] at assay	C H <sub>2</sub> O <sub>2</sub> in the reaction [μM]
6 mW/mm <sup>2</sup> , 5 ms pulse in 200 ms interval	Au	24.75	16.24	97.4
		50	6.79	81.6
	ITO	7	0	
		20		
	Au	12	2.70	16.2

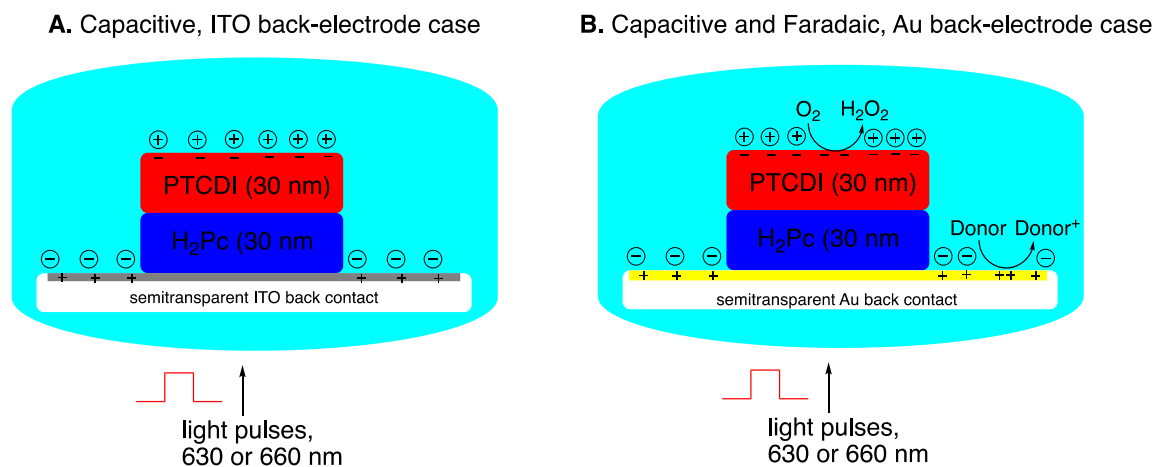


**Fig. S1. Illustration of photocapacitive versus photofaradaic behavior in OEPCs.** Illustration of the idealized photocapacitive case (A) when an ITO back electrode is used, where only two oppositely-charged double layers form upon photoexcitation. When the more catalytically-active Au is used instead of ITO (B), oxidation of various species in physiological medium becomes facile, which supports, in turn, cathodic reduction of oxygen to hydrogen peroxide on the PTCDI component of the OEPC. Registering the evolution of peroxide over time is a convenient quantification of faradaic behavior.

Supporting SEM images:

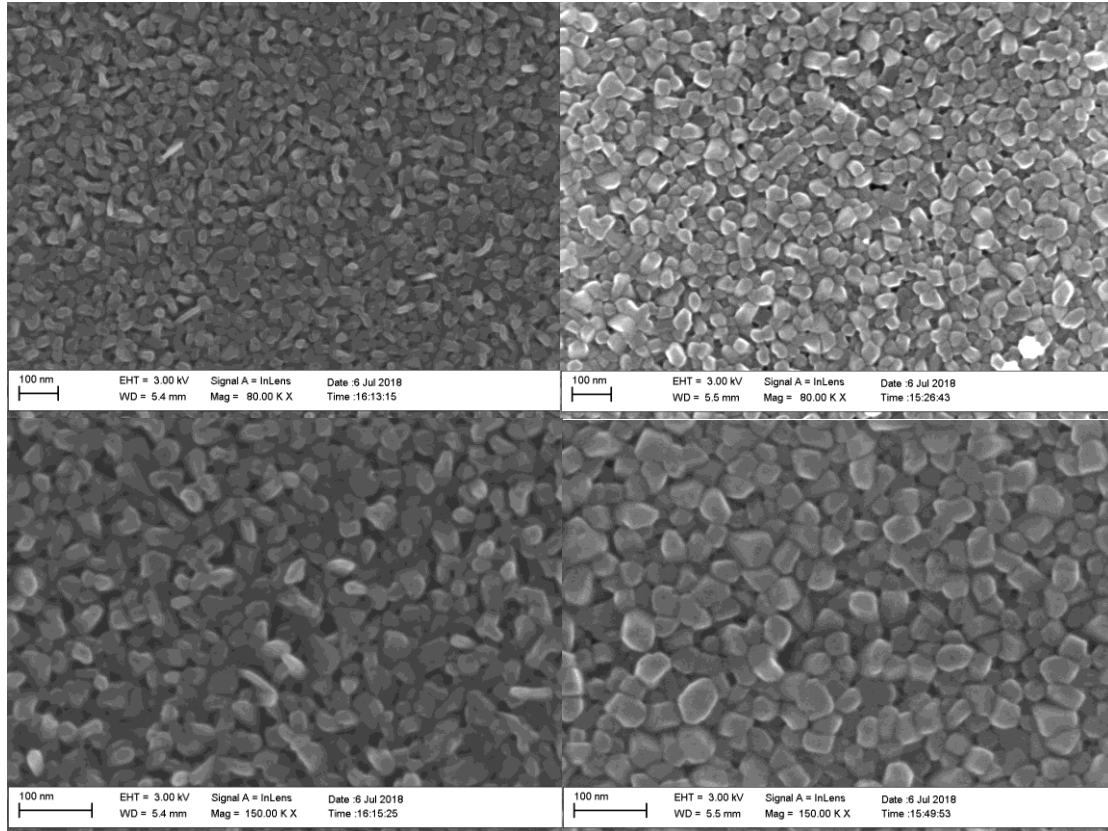


**Fig. S2. SEM micrographs comparing control samples of ITO/H<sub>2</sub>Pc/PTCDI. (left) and those treated with autoclave at 121 °C (right). All images taken after 35-day light stress test. A morphology change induced by autoclave is apparent in the shape and slightly larger size of the autoclaved sample crystals.**

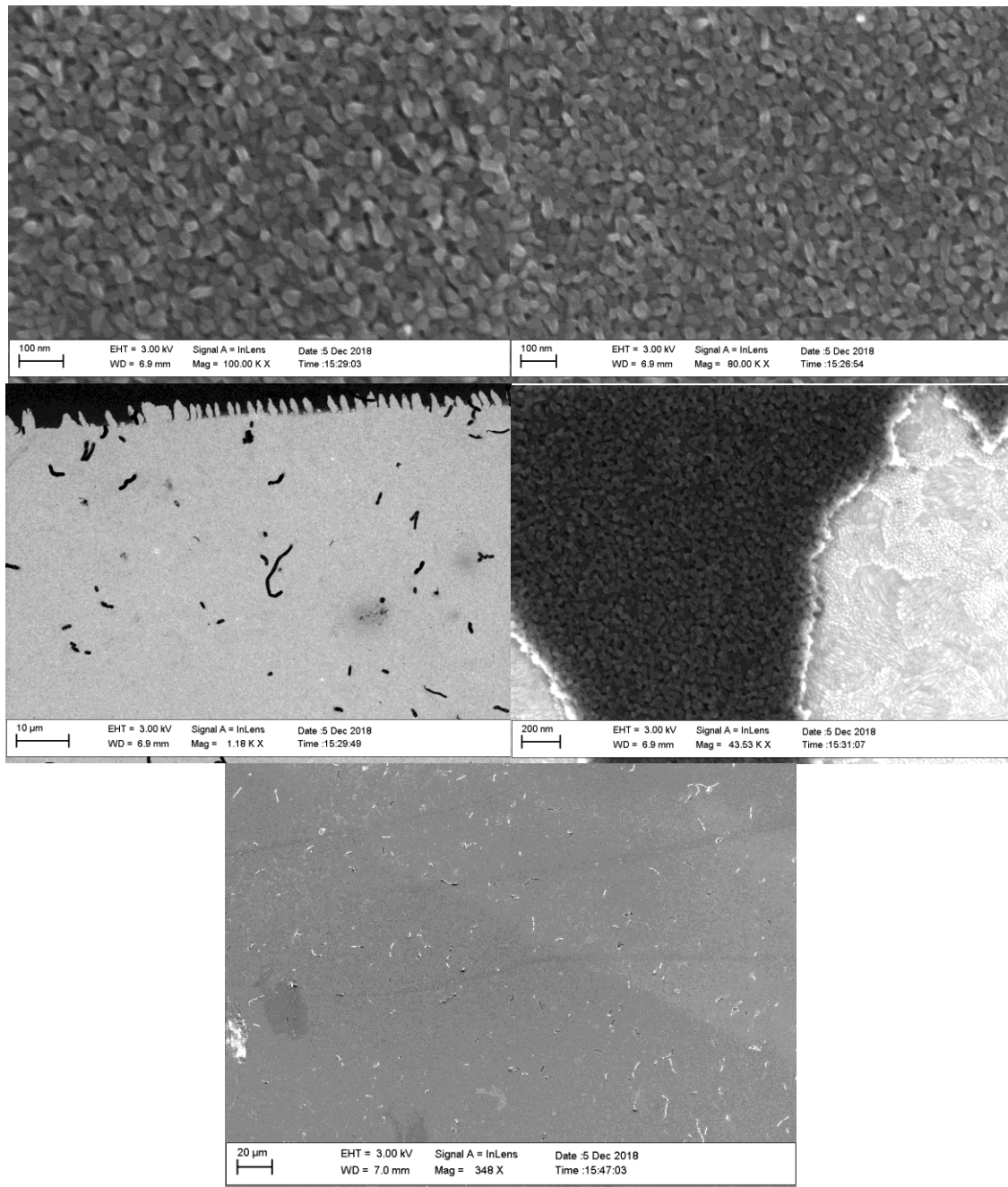


**Fig. S3. SEM micrographs of samples subjected to 178 days of light pulse stress.** The nanomorphology of all aged samples resembles that of autoclaved ones, demonstrating the clear effect of surface recrystallization in water. On the other hand, examination of the edges (middle row) shows that in some areas undercutting and delamination of the organic p-n layer is visible. This leads to pieces of organic material detaching and redepositing around the sample. The bottom image is an overview of an aged p-n area, showing pieces of delaminated material redeposited on the surface.

## Supporting Note 2. Numerical modeling of the OEPC/Oocyte interface.

The electrodynamic study of the photocapacitor/electrolyte/oocyte system was numerically computed in a pseudo-3D axisymmetric geometry using a finite element analysis software (COMSOL Multyphysics® version 5.3a, COMSOL INC.). A time-dependent study was conducted using the “Electric Currents” interface of the AC/DC module of the COMSOL software, which is used to compute electric field, current, and potential distributions in conducting media under conditions where inductive effects are negligible but the capacitive effects are accounted for. The COMSOL software solves a current conservation equation based on Ohm’s law using the scalar electric potential  $V$  as the dependent variable. In the time-dependent numerical study the dynamic formulations for both conduction currents and displacement currents are used

$$\begin{aligned}\nabla \cdot \mathbf{J} &= \mathbf{Q}_j \\ \mathbf{Q}_j &= -\nabla \cdot \frac{\partial}{\partial t} (\varepsilon_0 \nabla V - \mathbf{P}) - \nabla \cdot (\sigma \nabla V - \mathbf{J}_e) \\ \mathbf{J} &= \sigma \mathbf{E} + \frac{\partial \mathbf{D}}{\partial t} + \mathbf{J}_e \\ \mathbf{E} &= -\nabla V\end{aligned}$$

where  $\mathbf{Q}_j$  are the current sources,  $\mathbf{P}$  is the electric polarization vector,  $\mathbf{D}$  is the displacement current,  $\sigma$  is the electrical conductivity and  $\mathbf{J}_e$  are externally generated currents.

The electrolyte/oocyte/photocapacitor system was modeled in a 2D cross-section, in order to take advantage of the axial symmetry of the system. The photocapacitor was represented by a 4 mm diameter conductive disk with a very high contact resistivity ( $\rho = 10^{15}$  Ohm m<sup>2</sup>), to replicate the non-faradaic nature of the excitation. The conductivity of the disk and the applied potential to the disk were time-dependent, having “light” values (4 mS/m and -1.55 V) during the 1 ms light pulse and “dark” values (19 mS/m and 0 V) at other times. The surface capacitance of the disk was set to 1.8  $\mu\text{F}/\text{cm}^2$  (dark) and 2.3  $\mu\text{F}/\text{cm}^2$  (light). These values were obtained by starting from the best-known values for the system, which are known to be dependent on the light conditions, and by adjusting those values to obtain the best fit of the calculated intracellular potential in the oocyte to the measured values.

The disk was put in an electrically conductive medium (a circular right cylinder 5 mm in diameter and 3.5 mm in height, of electric conductivity of 1.25 S/m, grounded on the top and the sides) representing the electrolyte used in the oocyte experiments. The oocyte cell was modeled as a sphere of 1 mm in diameter, with a truncated flat zone 200  $\mu\text{m}$  in diameter at the bottom, representing the contact area with the photocapacitor. The model cell was placed at a distance of 3  $\mu\text{m}$  from the model-photocapacitor, a distance which we believe accurately represents the cleft width in the modeled system. The model cell was given a high surface resistance ( $\rho = 10^{13}$  Ohm m<sup>2</sup>) representing the lack of endogenous ion channels, a surface capacitance of 1  $\mu\text{F}/\text{cm}^2$  and the resting potential of -34 mV.

A 1 ms constant voltage pulse starting at 0.5 ms was applied to the disk, resulting in capacitive spatial currents in the electrolyte and the oocyte. To faithfully model the charging and discharging dynamics of the system due to the differing properties of the photocapacitor in the light vs. dark, the disk bulk conductivity and contact capacitance were fitted separately during the light-excitation phase and the “dark” part of the time-dependent study. The disk bulk conductivity, surface capacitance, and excitation voltage were initially set to match the measured injected current density (200-600  $\mu\text{A}/\text{cm}^2$ ) by the photocapacitor under the light intensity used in the experiment. The photocapacitor/electrolyte interface capacitance was set to the value (3-4  $\mu\text{F}/\text{cm}^2$ ) previously determined by electrochemical impedance spectroscopy. The parameters were further refined to match as closely as possible the measured intracellular voltage transient  $V_T$  from the inside of the oocyte. The response of the modeled system (the capacitive currents, resulting transient voltages and the changes in the cell membrane potential) to the voltage pulse representing the light excitation are shown in the main text (Fig. 3), and the supplemental video 1.

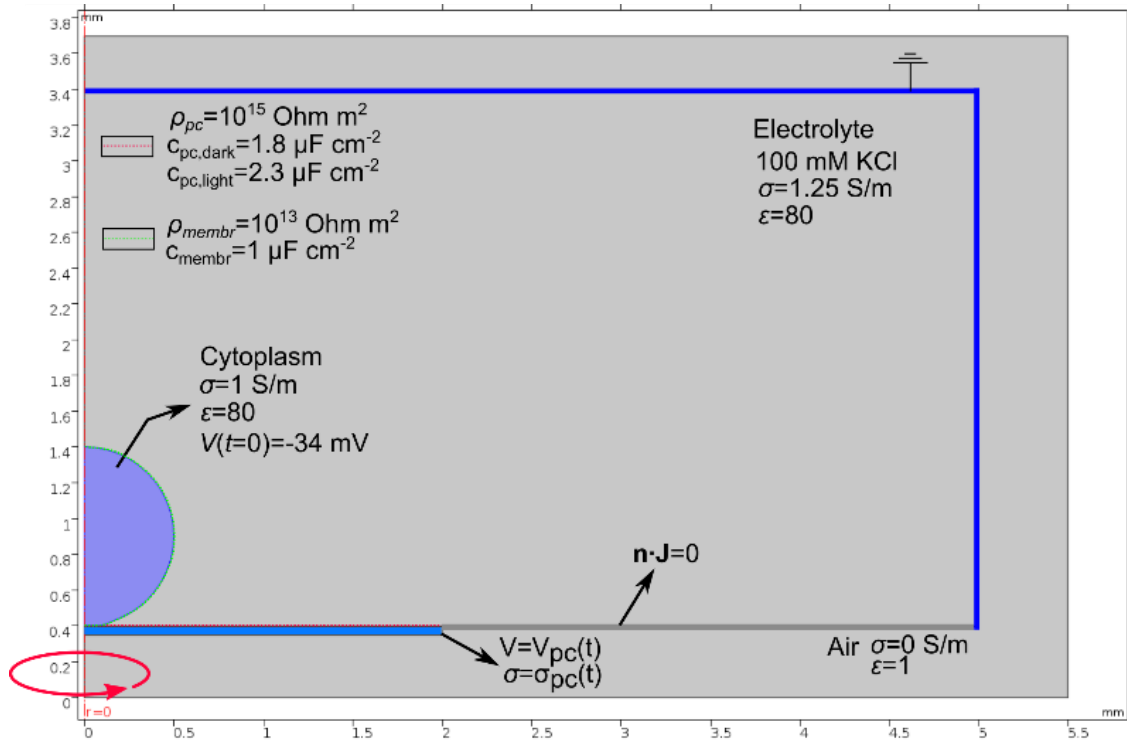


**Fig. S4. 2D representation of the electrolyte/oocyte/photocapacitor system.** Used for modeling of its electrodynamic response under the light excitation. Model parameters and boundary conditions are marked in the figure. The system possesses axial symmetry, which was used to compute a three-dimensional result with reduced computational cost.

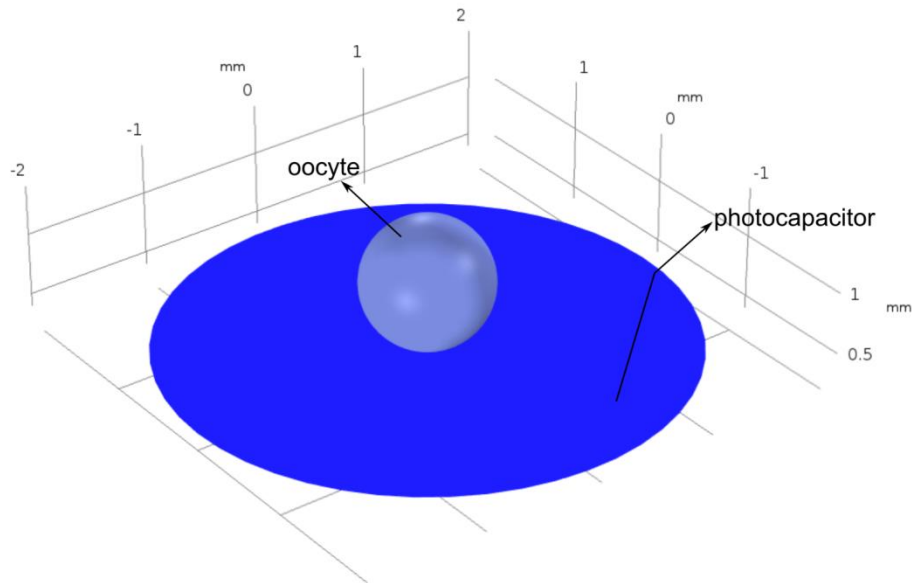


**Fig. S5. A 3D representation of the oocyte/photocapacitor model.** Obtained by rotating the two-dimensional axisymmetric model around the radial axis.

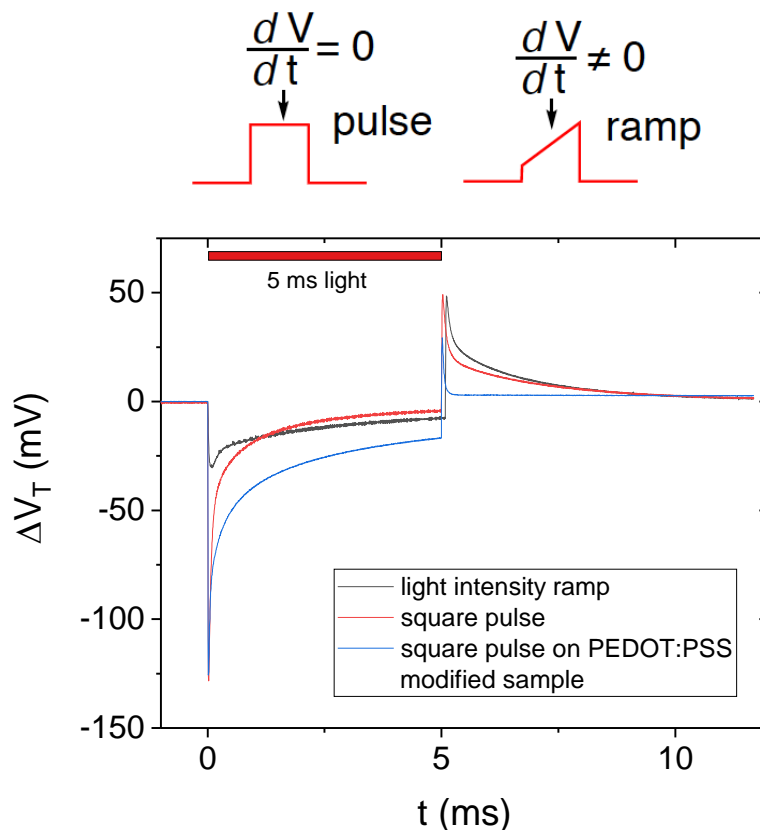


**Fig. S6. Comparison of voltage transients in the case of light intensity ramps with a standard square light pulse.** The ramping of the light intensity causes the derivative of charging current  $dI/dt$  to be nonzero, therefore the transient voltage in electrolyte persists. This is evident towards the end of the light ramp – the magnitude of voltage is higher than for the square pulse. Nevertheless, this performance is inferior to using PEDOT to increase the capacitance of the back electrode because the ramp technique does not increase the total photocharge the device produces during illumination. Despite the fact that for the experiment with voltage-clamp on potassium channels this was not ideal, the finding that light intensity ramps are an easy way to obtain a more flat, long-lived voltage transient is potentially useful.